

## INTERFEROMETRY WITH LARGE TELESCOPES

Pierre Léna

Université Paris 7 et Observatoire de Paris

92190 MEUDON France

1. Introduction. A popular - often textbook supported- view is that the diffraction limit of large telescopes is out of reach from ground-based observatories. We summarize on Fig.1 the scope of angular resolving power, in the range 100nm to 10.μm, as it appears today.

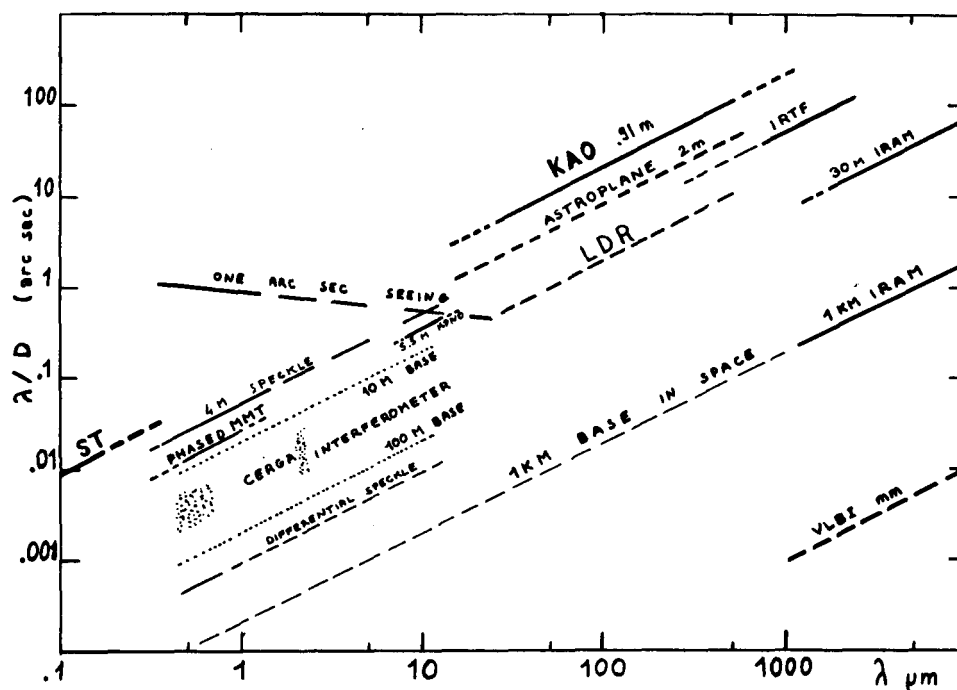


Fig.1. Angular diffraction limit  $\lambda/D$  versus wavelength for various telescopes (diameter  $D$ ) or interferometers (baseline  $D$ ).

A quick look reveals, expressed in absolute angular terms, a number of stimulating points :

(i) recent advances in *speckle techniques* allow to reach the diffraction limit of large ground-based telescopes, notwithstanding the seeing effects. Initially devised to measure double bright stars separation in the visible, these techniques have been extended to weak visible stars ( $m_v \sim 14$  to 16), to infrared sources (1-5 $\mu$ m), to full image reconstruction, and even to diffraction limited images obtained with optics suffering from residual aberrations (Faint Object Camera on the Space Telescope);

(ii) a promising development of speckle techniques is *the differential speckle method*, which allows a spatial resolution at least an order of magnitude beyond the diffraction limit (BECKERS, 1982) for some type of objects : the ones where two spatially separated points emit at two distinct wavelengths (such as opposite equatorial points of a rotating star, emitting red- and blue- shifted spectral lines);

*Proceedings of the IAU Colloquium No. 79: "Very Large Telescopes, their Instrumentation and Programs", Garching, April 9-12, 1984.*

(iii) the classical radio interferometry extends to millimeter wavelengths with large baselines, and successful attempts have been made to achieve interferometry on the same heterodyne principles in the infrared;

(iv) the Michelson direct interferometry, which is the ultimate method in terms of signal-to-noise ratio in the visible and in the infrared has now proven its feasibility with independent telescopes over long baselines. The CERGA interferometer, near Grasse (France), equipped with 1.5m telescopes should soon become fully operational, while the Multi Mirror Telescope (Mount Hopkins, Arizona) demonstrated the possibility to properly phase independent pupils carried by a single mount;

(v) a large gap still remains in the far infrared and submillimetric range, because of the atmospheric absorption. Currently discussed space missions, such as the Large Deployable Reflector, shall not fill this gap.

If the goal is to obtain a view of an astronomical object at comparable angular resolution between 100 $\mu$ m and 1000 $\mu$ m, many steps remain to be achieved. It is the purpose of this paper to examine how a ground-based large telescopes array could contribute to this goal. We restrict the discussion to interferometry, since other contributions to this Conference discuss various methods to achieve single pupil full resolution (speckle, differential speckle, active or adaptive optics).

2. Interferometry in Space. The main difficulties encountered by ground-based interferometry are due to the parasitic effects of the atmospheric turbulence and to the diurnal motion. It is therefore appropriate to set the standards of ultimate performances by a close examination of space mission capabilities. Only then would eventually be assessed the value of a ground-based large scale program.

The concept of a space interferometer is studied by Agencies, such as the TRIO study at the European Space Agency. It basically involves three satellites. Two of them carry telescopes, pointed at the object, a third one carries the common beam recombiner and detectors. Let  $O_\lambda(\alpha)$  be the object spatial structure,  $\alpha$  the angular variable on the sky,  $O_\lambda(W)$  its spatial spectrum (Fourier transform),  $D$  the projection of the interferometer baseline on the sky. The measured quantity is  $O_\lambda(W = \frac{D}{\lambda})$ . For a telescope diameter  $d$  much smaller than the baseline ( $d \ll D$ ), the measurement requires a single-pixel detector per spectral element: the information consists of a single "pixel" in the  $W=(u,v)$  frequency plane, it could be called a "Fourier" or Fourier element, a possibly useful neologism !

(i) for a perfectly stable baseline, one measures both amplitude and phase of the computed quantity  $O_\lambda(W)$ . Integration may be carried for any amount of time  $T$ , and the signal-to-noise improvement simply goes as  $T^{1/2}$ .

(ii) perturbations may reduce the baseline stability time to a maximum time  $\tau$ . Total observing time must be sub-divided. Long integration becomes less efficient, as limiting magnitudes will only improve as  $(T/\tau)^{1/4}$ . RODDIER (1983) has studied performances and limiting magnitudes of a space system in the visible (Fig.2), and demonstrated the value of this approach.

A similar examination has not yet been carried in depth at infrared wavelengths. The chief difference lies in the noise sources, as examined by RODDIER and LENA (1984) and detailed on Fig.3.

Signal photon noise is usually negligible and the goal is to be limited by detector noise. Background thermal noise overcomes it almost at any wavelengths beyond 2-3 $\mu$ m. In space, a considerable gain is therefore obtained by cooling the optics. Because, as we shall see below, it is expected that the atmospheric turbulence effects are manageable on the ground in the infrared, one immediately concludes that a space-borne interferometer will represent a significant gain over a ground-based system :

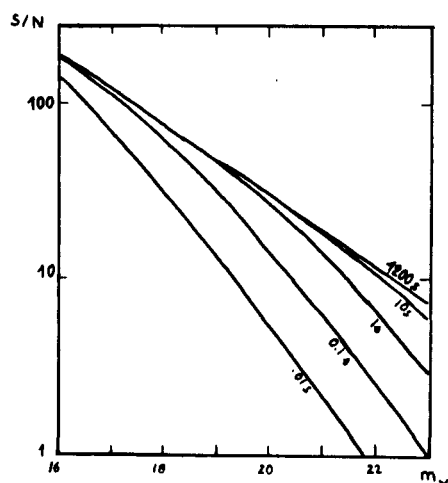


**Fig. 2** Signal-to-noise versus magnitude  $m_v$ , as obtained with a space-borne interferometer. Stability time  $\tau$  of the baseline is indicated.

Area =  $1 \text{ m}^2$ .

Quantum efficiency  $\eta = 0.2$

Bandwidth  $\Delta\lambda = 60 \text{ nm}$ . Total integration time  $T = 20 \text{ mn}$ . (RODDIER, 1983).

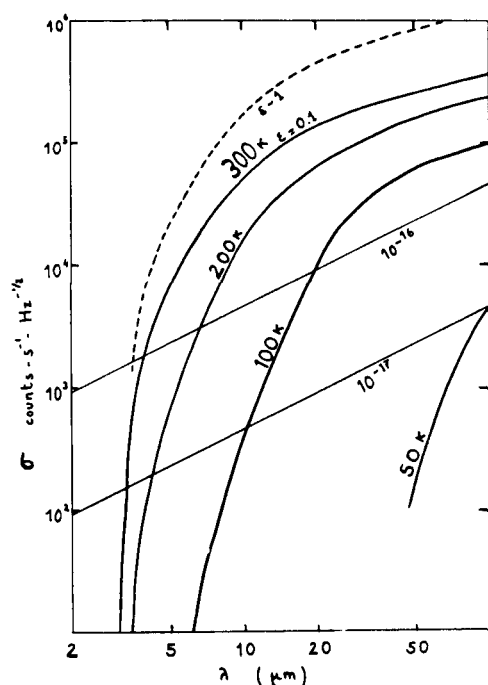


**Fig. 3.** Dominant noise sources in the infrared. The straight lines are typical detector noise figures, for NEP of  $10^{-16}$  and  $10^{-17} \text{ W.Hz}^{-1/2}$ . Ordinates are in units of counts  $\cdot \text{s}^{-1} \cdot \text{Hz}^{-1/2}$ . The curves give the background thermal noise for various temperatures of the optics (50 to 300 K) and emissivity  $\epsilon = 0.1$ . The dotted curves is related to the worst case of ground-based observations, where the emissivity would be close to unity. The following assumptions have been made : noise is measured in a diffraction-limited throughput  $S \Omega = \lambda^2$ , hence the result is independent of telescope diameter and field of view. Quantum efficiency of detectors : 0.5  
Bandpass  $\Delta\lambda / \lambda = 0.1$

- (i) shortward of  $2\text{--}3 \mu\text{m}$ ;
- (ii) even in atmospheric transmission windows ( $\lambda < 30 \mu\text{m}$ ) if it is equipped with cooled optics;
- (iii) longward of  $30 \mu\text{m}$ , with either warm or cooled optics, the latter being a considerable improvement over the former.

Conversely, a ground-based system, working in the atmospheric windows, presents little degradation over an uncooled space system.

**3. Ground based interferometry.** The feasibility of beam combination and visibility measurements is now proven in the visible as well as in the infrared, using either two telescopes on the same mount (MMT configuration) or independent telescopes (Labeyrie's approach).

Compared with the very simple situation encountered in space, ground based

observations suffer from a severe degradation due to the atmospheric turbulence. The accuracy which can be achieved on the measurement of the source spectrum  $O_\lambda(W)$  - both in amplitude and phase- is limited, as will therefore be limited the reconstruction of a synthesized aperture image from properly sampled values of  $O_\lambda(W)$ .

A general discussion and references may be found in RODDIER and LENA (1984).

Fig.4 shows a particular configuration, which well illustrates the general features of recombined image in presence of turbulence : existence of speckles, high spatial frequency fringes in overlapping speckles, random phase of fringes from speckle to speckle, time evaluation of the whole random pattern. It can be shown (RODDIER, LENA, 1984) that the high frequency spectral density of the image is related to the source spectrum by a relation of the type

$$\frac{\text{image spectral density at fringes frequency}}{\text{image spectral density at origin}} = A \left| \frac{O_\lambda(W)}{O_\lambda(0)} \right|^2$$

In the absence of turbulence (e.g. in space),  $A = 0.5$ . In the presence of turbulence,  $A$  becomes a random quantity varying with time, and averages need to be taken in order to extract the object spectrum modulus. The result generally depends on turbulence parameters, such as the Fried parameter  $r_0$ , or the outer scale of turbulence. Hence the accuracy on  $O_\lambda(W)$  shall be limited, but fortunately it can be shown that a remedy lies in image motion stabilization before to recombine the beams.

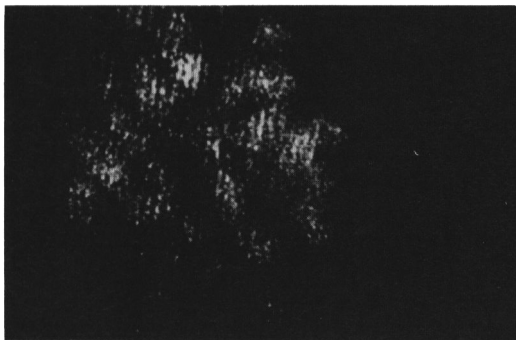


Fig.4. Coherent superposition of two telescopes images. Two pupils of the Multi-Mirror Telescope are phased in order to obtain equal optical paths from the source (a star) to the common focus of the telescope. Wherever speckles overlap, fringes are observed. Note the random character of the speckles superposition, and the random phase of fringes from speckle to speckle.  $\lambda = 600 \text{ nm}$

Exposure rate set by the TV rate of 60 images  $\cdot s^{-1}$ . (This unpublished result is due to the courtesy of J.BECKERS and N. WOOLF).

If this is done, taking proper averages on the left-hand side quantities leads to  $A = 0.5$  : one recovers a turbulence-free situation, as far as spectrum modulus is concerned. Considerable experience gained in infrared speckle interferometry during the last years (CHELLI, 1984) has shown that such approaches can be successful and lead to very accurate determination of the object spectrum, as long as great care is exercised in the data acquisition and analysis.

Full image reconstruction cannot be obtained without the knowledge of the phase  $\phi_\lambda(W)$  of the complex quantity  $O_\lambda(W)$ . Atmospheric random phase fluctuation shall probably prevent a direct determination of  $\phi$ , at least at visible wavelengths and with large telescopes. Indirect methods of phase reconstruction have been devised by radio-astronomers (phase closure) or, more recently, for speckle data analysis (Knox Thomson, Fienup, Walker algorithms). They have all in common to require the knowledge of  $|O_\lambda(W)|$  with a good signal-to-noise ratio and a fairly complete, two-dimensional coverage of the frequency  $W$ . Recent results obtained in speckle interferometry, both in the visible (RODDIER and RODDIER, 1984; WEIGELT, 1984) and in the infrared (CHELLI, 1984) again show that this approach can be fruitful.

The infrared case for ground-based interferometry is especially appealing, given the fact that large telescopes remain almost diffraction limited, even in

the presence of atmospheric turbulence (Table I). Indeed the behavior of all turbulence-induced parameters is favorable : the wavelength dependance of the Fried parameter  $r_0$  ( $\propto \lambda^{6/5}$ ), of the atmospheric correlation time ( $\propto \lambda^{6/5} \tau_0$ ), of the acceptable spectral band pass ( $\Delta\lambda \propto \lambda^2$ ), of the phase r.m.s. excursion between two pupils located on a base line  $D$  ( $\sigma \propto \lambda^{-1}$ ), of the image isoplanetic domain ( $\propto \lambda^{6/5}$ ). We shall therefore restrict the following discussion to the infrared case.

TABLE I

Average Number of Speckles in the Image

Seeing (at 0.5 $\mu$ m)		$\lambda$ ( $\mu$ m)				
		2.2	3.5	5	10	20
<u>D = 1.5m</u>	2"	59	19	8	A	A
	1"	15	5	2	A	A
	0.5"	4	A	A	A	A
<u>D = 4m</u>	2"	420	138	59	11	2
	1"	105	35	15	3	A
	0.5"	26	9	4	A	A
<u>D = 8m</u>	2"	1680	551	234	44	8
	1"	420	138	59	11	2
	0.5"	105	35	15	3	A

(A) means Airy disc, i.e. an almost perfectly diffraction - limited image, when  $r_0 \gg D$ .

The infrared case. The aim of the present discussion is to establish what would be the capabilities of the interferometric mode of a large-telescope interferometer on the ground. To achieve high sensitivity and proper image reconstruction, many technical steps have to be carried; they will be shortly discussed, and are summarized on the flow-chart presented on Fig.5. The basic interferometric configuration is described on Fig.6. Although many variations are possible, it contains the essential features of the analysis of a combined image, namely the choice between single pixel or multi-pixel detector.

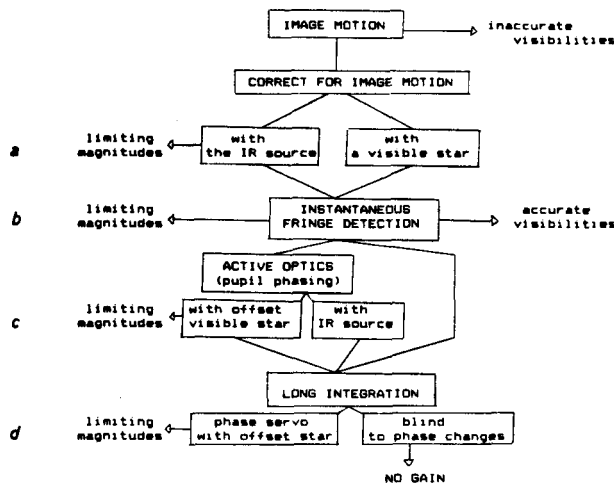


Fig.5. Flow-chart describing the steps toward an accurate measurement of the object spectrum  $O_\lambda(W)$ . The letters a/ to d/ refer to paragraphs in the text.

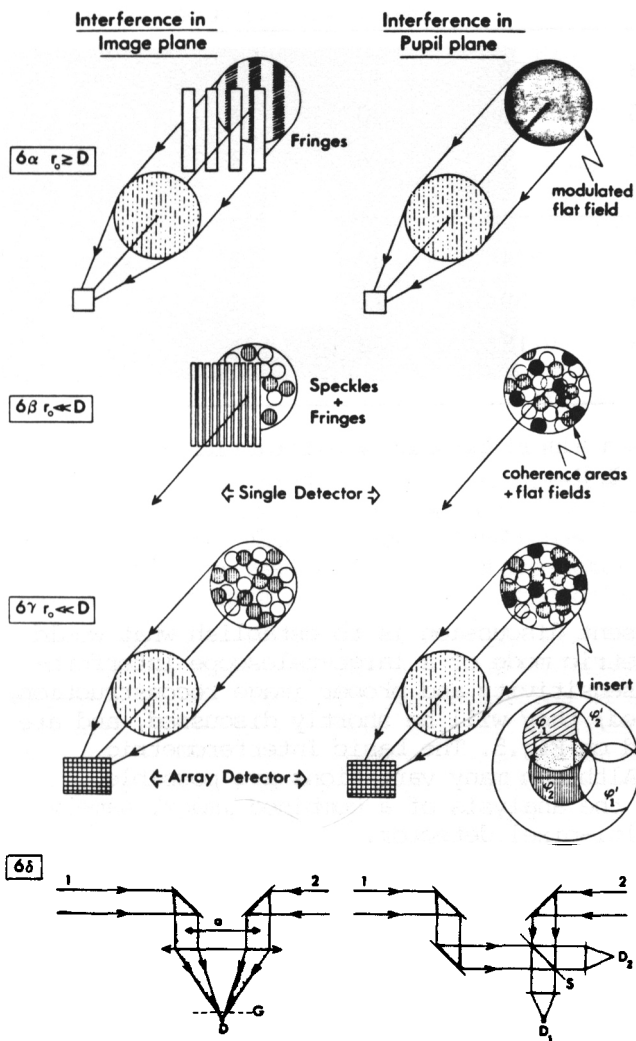


Fig.6. Combining beams in a common interferometric focal plane. Interference pattern in the image plane (left column) or pupil plane (right column).  $D$  is pupil diameter. Single detector is used when  $\alpha/r > D$ ,  $\beta/r \ll D$ . A grid is used to detect the fringes contrast.  $\gamma/r \ll D$ . Array detector. Focal plane or pupil plane are focused on the detector. The insert shows coherence areas of respective phases  $\phi_1$  and  $\phi_2$ , given by the two pupils, superimposed and giving the flat field over the pixel.  $\delta$  / Optical arrangement (schematic). Left: the distance  $a$  fixes the fringe spacing. Right: afocal beams are focused on Detectors 1 and 2 after combining through a beam splitter  $S$ . Pupil images are on detectors.

a) As discussed above, the first step is *image stabilisation*. Correcting in real time for the image motion induced by the atmosphere is rather simple. The most general assumption is that the source under investigation has no visible counterpart. The factor setting the limiting fluxes is the atmospheric correlation time. Using current infrared detectors performance, it is easy to deduce the limits of a stabilisation system for various telescope diameters. Although Fig. 7 shows that these limits are fairly satisfactory with respect to the objects to be studied, improvements may be obtained: it can be shown that image motions are highly correlated over fields of view as large as 2' or 3', the correlation being practically achromatic. Hence, one may use a visible field star close enough to the IR source to derive the stabilisation error signal.

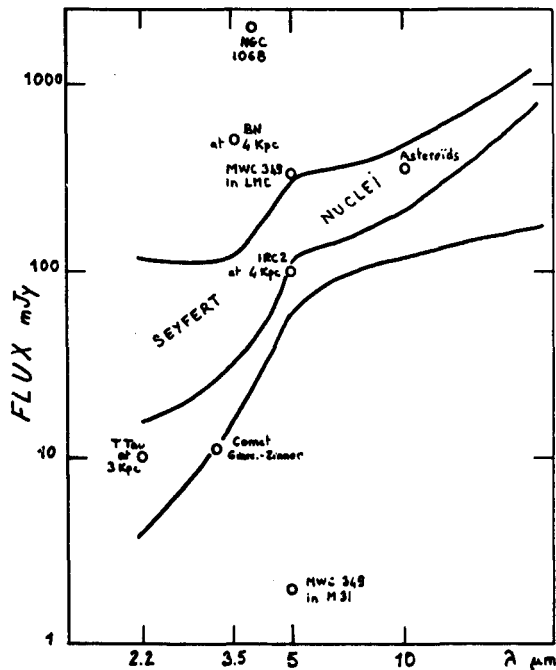


Fig. 7. Flux limits for image stabilisation, with various telescope diameters. The following assumptions have been used: transmission  $\times$  quantum efficiency = 0.3; detector noise  $\sigma_R = 10^4$  counts  $s^{-1} Hz^{-1/2}$ . Signal/noise = 5. Atmospheric correlation time = 20 ms at 500 nm;  $r_0(0.5 \mu m) = 10$  cm; Field of view = 2 arc sec.

For comparison, a number of objects have been reported on the diagram.

b) the next step is *fringe detection*. As long as this measurement is attempted on a single frame, i.e. within the atmospheric correlation time, the bandwidth (or temporal coherence) requirement aims simply to maintain coherence over the pupil (Fig. 8). The visibility measurement on a single frame may be carried either with a single detector, or with a detector array (imaging capability). Although the latter is not requested when the image contains a single speckle, it becomes necessary for large pupils and/or short wavelengths, otherwise a net loss of contrast would result from fringes averaging. The limiting fluxes are shown on Fig. 9, and are to be compared with the ones obtained in step a/ above.

Two facts are striking: without array detectors, the use of a large telescope gives worse results, a fact which is the direct consequence of detector mismatching. The use of an array improves the performances, but only beyond  $5 \mu m$ . The photon collection potential of a very large telescope is not exploited properly at short wavelengths, because of the read-out noise of arrays: breaking the image in small pixels increases the overall equivalent detector noise. Yet, within these limits, accurate measurements of the visibility, i.e. of the quantity  $|O(W)/O(O)|$ , may be obtained. Some improvements (at most a factor 5 to 10) may result from the time integration of a few frames, at least when the

fringes sweeping rate due to wind and turbulence remains low (MARIOTTI, 1984).

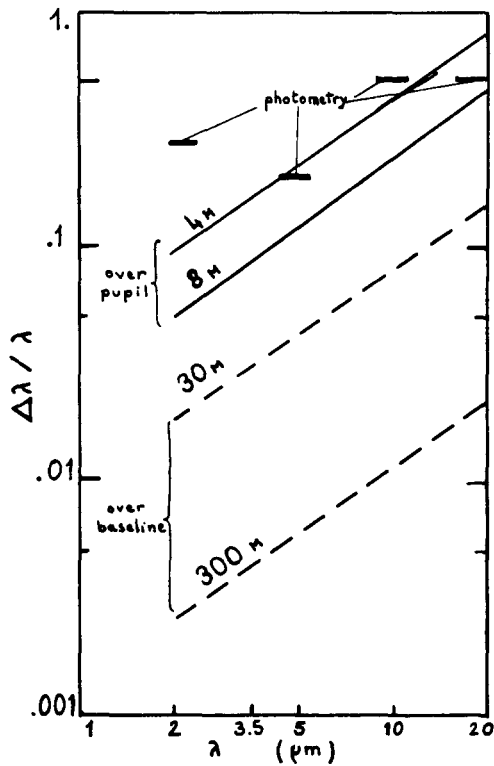


Fig.8 Bandwidth (or temporal coherence) versus wavelength for different requirements. Above : standard photometric bandpasses, as set by the atmospheric transmission. Full : coherence over pupil only. Dotted : coherence maintained over baselines (D = 30 to 300 m). In the two latter cases, the phase dispersion is due to the atmospheric turbulence.

c) to overcome the sensitivity loss due to the scatter of information on many pixels of an array, and to the subsequent read-out noise, it is appropriate to reduce the image size given by either telescopes, i.e. to phase the pupil. Would such a goal be obtained, a significant sensitivity gain results (Fig.9), and the potential of large telescopes becomes clear.

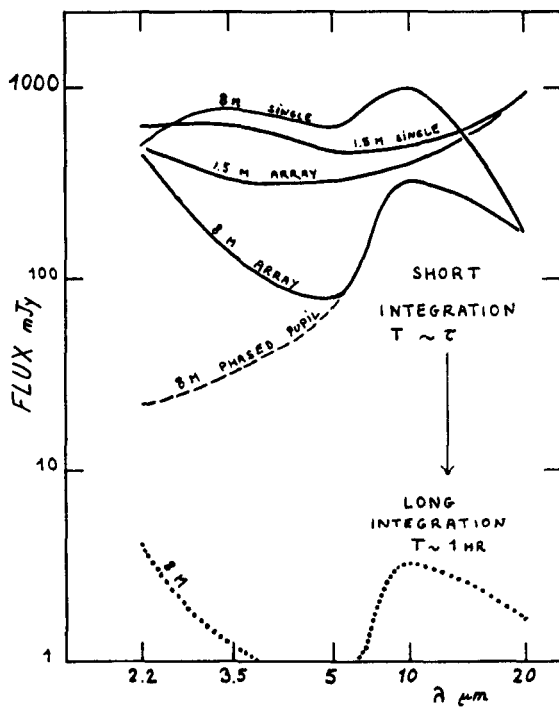


Fig.9. Flux limits for instantaneous fringe detection, on same scale as Fig.7. Observational parameters are identical to the ones from Fig.7



Phasing the pupil in real time requires active optics. Fortunately, in the infrared, the number of phase cells remains modest even over large pupils (Table I). The main difficulty is the derivation of the error signal : it may indeed be done from the source signal itself, but this would not bring any sensitivity gain. Another approach is to take advantage of the large isoplanetic field in the infrared (several arc min at  $20\mu\text{m}$ ); if a visible star lies within this field, one expects the low spatial frequency phase excursion over the pupil to be highly correlated with the phase excursion over the pupil in the infrared. Hence, the information derived from the visible star may be used to generate the error signal needed by the active optics controls. Preliminary computations show that a visible star  $m_V \approx 14$  should be bright enough to achieve this result. The phasing of the pupil then becomes independent of the IR source flux and a drastic noise reduction follows, especially for large telescopes, as illustrated on Fig.9.

d) the fourth step is to achieve long time integration to measure visibilities on weaker sources. As time goes, random phase shifts, due to atmospheric turbulence, occur between the wave fronts reaching the two pupils. At first glance, these phase shifts cannot be monitored since the signal-to-noise ratio per frame becomes less than unity for a weak source. Long integration can only be carried by averaging spectral densities of individual frames, while the temporal coherence over the whole base line is requested (Fig.8), further reducing the signal. It can then be shown that no sensitivity improvement is obtained from long integration.

The only way to improve the sensitivity lies in monitoring atmospheric (and possibly instrumental and/or tracking) phase drifts. Spectral densities averages are then replaced by complex spectrum averages, and flux limits would improve with integration time as  $T^{1/2}$  rather than as  $T^{1/4}$  in the above case. This last step, illustrated on Fig.9, opens an extremely wide range of objects to investigation. Yet, achieving it is a difficult challenge, since it requires phase drifts monitoring over a brighter IR source, or a visible source, within the isoplanetic field, but at the common interferometric focus. This common focus is not expected to present any field of view since it is fed by afocal beams. Hence this approach may require rather complicated optical lay-outs.

All the above consideration only lead to the knowledge of the spectrum modulus  $|O_\lambda(\mathbf{W})|$ , or to a similar quantity, the fringes visibility of the object. It is quite obvious from radio astronomy aperture synthesis and infrared speckle interferometry that a good sampling of the frequency plane is required to derive useful astrophysical information. As an example, we illustrate on Fig. 10 the frequency coverage which would result from a configuration of a possible array, similar to the one presented by ENARD (1984).

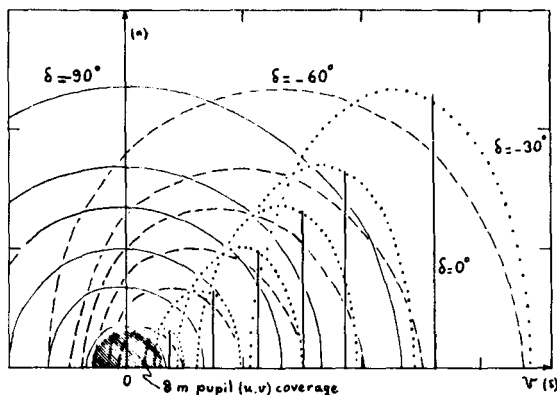


Fig.10 . Spatial frequency coverage of a linear array, using supersynthesis by Earth rotation. 4 telescopes, 8m diameter, are aligned with spacings of 40, 20 and 80 meters between neighbouring telescopes. A baseline at  $45^\circ$  of the N-W direction is chosen at a latitude  $20^\circ$  South. Declination of source is indicated.

At this point image reconstruction can be achieved if relative phases of the quantities  $\tilde{O}_\lambda(W)$  are known with respect to  $\tilde{O}_\lambda(O)$ . Phase closure methods may be used, but this requires simultaneous observation by more than two telescopes. Extrapolation of well-practiced radioastronomy methods obviously requires further investigation. It should be noted that the atmospheric phase r.m.s. excursion increases only up to the outer scale of turbulence. A site measurement of this quantity is an important criterion for interferometry.

4. Concluding remarks. In summary, we have shown that ground-based interferometry with large telescopes has a significant potential, especially in the infrared, where the comparison with space-borne instruments is favorable, at least in a foreseeable future. Although limited to atmospheric windows short of  $30\mu\text{m}$ , there is a great wealth of astrophysical problems to be investigated : it is worth noting that a large telescope in an interferometric mode would not only give access to compact objects in the Galaxy, but also to a wide range of nuclei of galaxies.

The choice of site is crucial, not only in the trivial terms of atmospheric transparency, but also on the seeing quality ( $r_0$ ), on the atmospheric correlation time and on the outer scale of turbulence at and above the site.

Many points remain to be investigated in detail before the concept of large telescopes interferometry can be firmly assessed : effects of thermal background modulation, pupil phasing with an offset visible star, phase behavior over decametric baselines ... These studies, as well as first astrophysical observations, are currently planned with the two 1.5 m spherical telescopes built by A.LABEYRIE (1981) at CERGA, for which an infrared focal plane beam combiner is under construction (Fig.11).

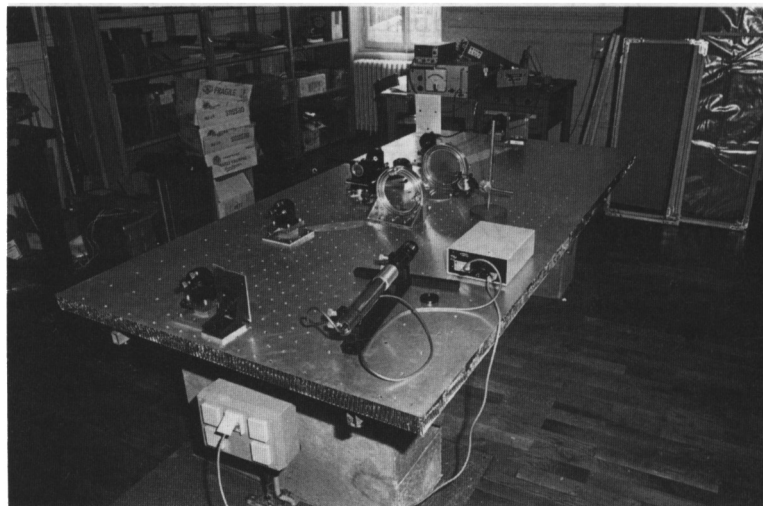


Fig.11. The infrared interferometric table under construction at Observatoire de Lyon. Two afocal beams are fed on the table; a dichroic selects a fraction for the energy for image stabilisation using an  $8 \times 8$  InSb CID array to generate the error signal. Beam recombination is made by superimposing pupil images on a single detector. (Courtesy J.M.MARIOTTI).

REFERENCES

- BECKERS J.M. *Opt. Acta.* 1982, 29, 361.
- CHELLI A. 1984. *Infrared Speckle Methods*, in this Conference Proceedings.
- ENARD D. "The Linear Array Concept", in this Conference Proceedings.
- LABEYRIE A. "Scientific Importance of High Angular Resolution at Infrared and Optical Wavelengths". p.225. ESO Conference, Garching 1981.
- MARIOTTI J.M. *Optica Acta.* 1983. 30, 831.
- RODDIER C., RODDIER F. *Ap. J.* 1983, 270 , L23.
- RODDIER F. *Adv. Space Res.* 1983, 2, 3.
- RODDIER R., LENA P. *Journ. of Optics.* 1984. In press.

DISCUSSION

J.E. Noordam: I would like to point out that image reconstruction from the visibility-amplitudes alone (Fienup, etc.) is only possible if the UV-plane is fully sampled. This is not usually the case for aperture synthesis arrays, especially at optical/IR wavelength. In these cases one needs phase-closure techniques like in Very Long Baseline (Radio) Interferometry.

P. Lena: I fully agree with you. In fact, your point is a strong argument to conceive the IR/optical array as one which has the capability to cover the UV plane in a filled manner, up to the maximum frequency.